iScience

CellPress
OPEN ACCESS

Article

Trigeminal nerve-derived substance P regulates limbal stem cells by the PI3K-AKT pathway

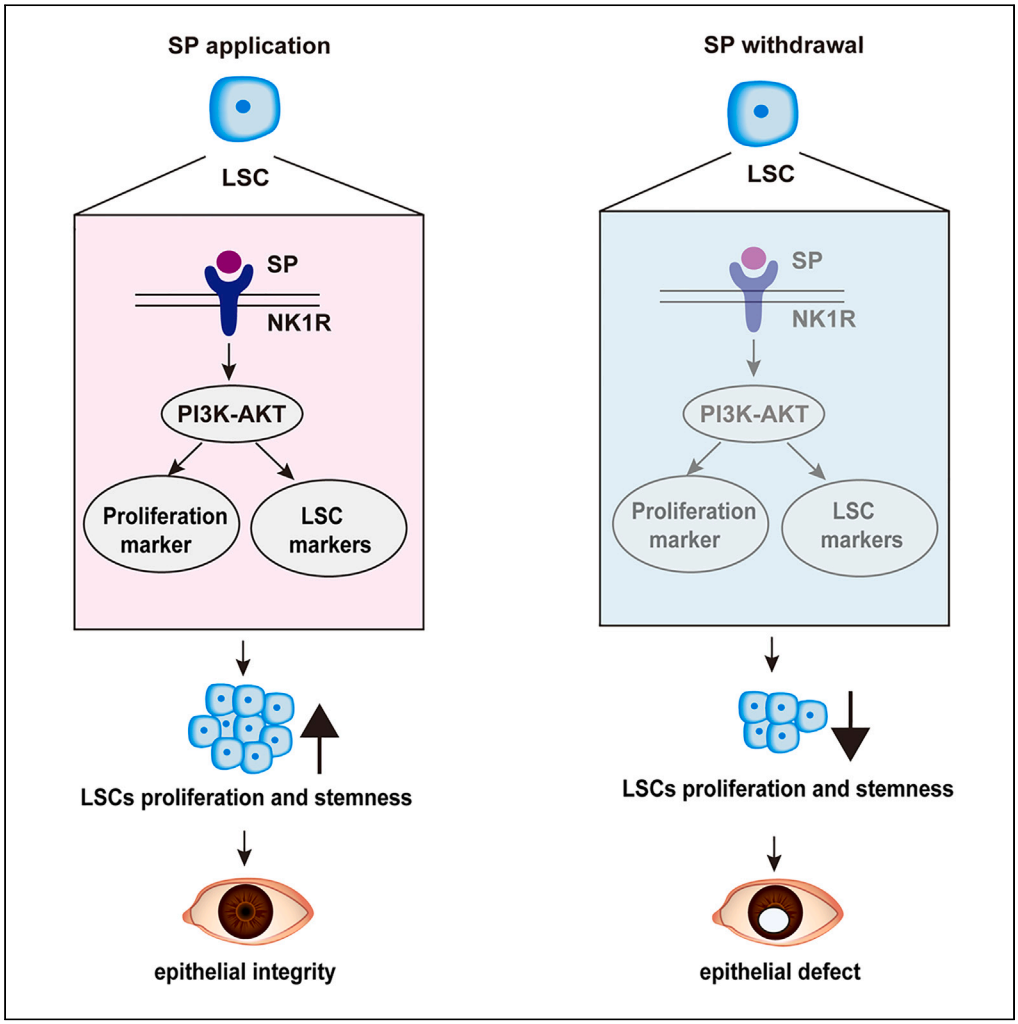

Peipei Xu, Xiongshi Lin, Xing Dong, Ying Liu, Zhichong Wang, Shuangyong Wang

wangzhichong@gzzoc.com (Z.W.)
364853063@qq.com (S.W.)

Highlights

Trigeminal nerve is vital to regulate limbal stem cells

The level of substance P is reduced in corneal denervation mice

Substance P regulates the proliferation and stemness of limbal stem cells

Substance P regulates limbal stem cells by the PI3K-AKT pathway

Xu et al., iScience *26*, 106688
May 19, 2023
https://doi.org/10.1016/j.isci.2023.106688

iScience

CellPress
OPEN ACCESS

Article

Trigeminal nerve-derived substance P regulates limbal stem cells by the PI3K-AKT pathway

Peipei Xu,[1] Xiongshi Lin,[1] Xing Dong,[1] Ying Liu,[2] Zhichong Wang,[2,*] and Shuangyong Wang[1,3,*]

SUMMARY

Trigeminal nerve-derived substance P (SP), a widespread neuropeptide, is known to maintain the corneal epithelial homeostasis and promote the closure of wound healing. Using comprehensive *in vivo* and *in vitro* assays and RNA-sequencing analysis, we aimed to unveil the positive effects of SP on the biological characteristics of limbal stem cells (LSCs) and the underlying mechanism. SP enhanced the proliferation and stemness of LSCs *in vitro*. Correspondingly, it rescued corneal defects, corneal sensitivity, and the expression of LSC-positive markers in a neurotrophic keratopathy (NK) mouse model *in vivo*. Topical injection of a neurokinin-1 receptor (NK1R) antagonist caused similar pathological changes as in corneal denervated mice and attenuated LSC-positive markers levels. Mechanistically, we revealed that SP regulated LSCs functions by modulating the PI3K-AKT pathway. Our findings showed that the trigeminal nerve regulates LSCs by releasing SP, which may provide new insights into the regulation of LSCs' fate and stem cell therapy.

INTRODUCTION

Limbal stem cells (LSCs) residing in the corneal limbus are the main source of replenishment for corneal epithelial cells through self-renewal, differentiation, and migration. LSCs are supported and regulated by the limbal niche, a special microenvironment, that consists of cells, extracellular matrix, and signaling molecules.[1,2] Dysfunction or deficiency of LSCs can result in corneal epithelial defects, corneal neovascularization, and inflammation, which may cause severe visual loss, even blindness.[3] However, the critical molecules and mechanisms that regulate LSCs functions are poorly understood. Neuropils can regulate the niche microenvironment of adult stem cells (ASCs) by releasing neurotransmitters or neuropeptides, thus maintaining the proliferation or differentiation of ASCs.[4–6] Neuropeptide F is a vital factor to regulate the proliferation of germline stem cells in *Drosophila melanogaster*.[5] During development, parasympathetic innervation maintains undifferentiated keratin 5-positive epithelial progenitors in the salivary gland.[7] Therefore, similar to the ASCs, one important way to investigate the biological regulation of LSCs is to understand how they are regulated by their niches and the released neuropeptides.

The cornea is densely innervated by the ophthalmic branch of the trigeminal nerve, entering the cornea at the limbus and penetrating into the corneal epithelium.[8,9] Correspondingly, the limbus, where LSCs reside, also has dense nerve distribution,[10,11] suggesting the potential role of nerve fibers in LSCs. Herpetic infection, neurosurgical sequelae, and diabetes may cause impairment of the trigeminal nerve and corneal innervations, leading to neurotrophic keratopathy (NK).[12,13] In a mouse model of NK, the number of LSCs was significantly reduced, and the levels of LSCs markers were decreased, suggesting that corneal nerves are vital to regulate stem cells and their niches.[11] Interestingly, the absence of a trigeminal nerve-released neurotrophic factor, substance P (SP), was supposed to cause NK.[13] SP is released predominantly by nerve fibers and functions mainly through interactions with NK1R.[14] In the cornea, SP-NK1R interaction promotes the closure of wound healing,[15] which relies on the differentiation, migration, and proliferation of LSCs.[1] During the progress of corneal wound healing, SP activates protein kinase, and integrin,[16] which are vital on the differentiation of LSCs.[17] In addition, SP regulates the differentiation of corneal epithelium and increases N-cadherin expression.[18] Importantly, N-cadherin is not only a positive marker of LSCs but also a vital adhesion molecule mediating the interaction between LSCs and the limbal niche.[19] These results suggest important roles for trigeminal nerve-released SP in regulating the biological characteristics of LSCs and the limbus niche microenvironment.

[1]The Third Affiliated Hospital of Guangzhou Medical University, Guangzhou, Guangdong Province, China

[2]State Key Laboratory of Ophthalmology, Zhongshan Ophthalmic Center, Sun Yat-sen University, Guangdong Provincial Key Laboratory of Ophthalmology and Visual Science, Guangzhou, Guangdong Province, China

[3]Lead contact

*Correspondence: wangzhichong@gzzoc.com (Z.W.), 364853063@qq.com (S.W.)

https://doi.org/10.1016/j.isci.2023.106688

In our study, we found that SP is a vital factor in maintaining the biological characteristics of LSCs. In a mouse model of NK, the level of SP decreased markedly in the corneas. However, SP enhanced the proliferation and stemness of LSCs *in vitro*. SP rescued corneal defects, sensitivity, and expression of LSCs markers *in vivo*. In addition, topical injection of an NK1R antagonist L-733,060 caused pathological changes similar to those in corneal denervated mice, particularly the attenuation of LSC-positive markers levels. In the literature, inhibition of AKT activity impairs the cloning formation of LSCs, suggesting that AKT signaling has important roles in LSC self-renewal.[20] However, there is no evidence that SP-NK1R interaction could regulate AKT signaling on LSCs. In our study, RNA-sequencing analysis revealed that the injection of the NK1R antagonist causes transcriptome-wide downregulation of genes of the PI3K-AKT signaling pathway. Mechanistically, SP-NK1R interaction affected LSCs via the PI3K-AKT pathway, and blocking this pathway diminished the positive effects on LSCs. Finally, our study reveals the mechanisms that regulate the biological characteristics of LSCs and may provide therapeutic target for LSCs transplantation.

RESULTS

Corneal denervation reduces SP level

To recapitulate the role of SP in LSCs, we constructed an experimental NK mouse model by transecting the ciliary nerves as previously described.[21] In fluorescein sodium staining and whole-mount corneal staining, the corneal epithelial defect was obvious. In the denervated mice, the density of corneal nerve fibers decreased significantly after 1 week of denervation treatment (Figure 1A). Coincidently, the corneal epithelial thickness of denervated mice was thinner than that of control mice (Figures 1B and 1C). In addition, immunohistochemistry staining showed that the expression of proliferation marker Ki67 was decreased in the limbus of denervated mice. The result reflected that denervation treatment weakened the proliferation of LSCs (Figure 1D). In the limbal tissues of denervated mice, the expression of LSCs markers such as N-cadherin,[22] ABCG2,[23] Bmi-1,[24] p63,[25] integrin α9 (Itga9),[26] and cytokeratin 15 (CK15)[27] (Figures 1E–1G) which are associated with the proliferation and self-renewal of LSCs decreased significantly.[28] However, the level of a specific corneal epithelial cell marker, cytokeratin 3 (CK3),[29] was upregulated (Figures 1F and 1G), indicating a differentiated state of LSCs. In addition, *in situ* hybridization was performed on histological sections at normal and denervated mice limbus. It showed that the expression of ABCG2, P63 transcripts on limbal region was decreased. On the contrary, the level of the corneal epithelial cell marker, cytokeratin 12 (CK12),[30] was upregulated (Figure 1H). These results implied that corneal denervation attenuates LSCs proliferation and stemness. In addition, in denervated mouse corneas, SP levels were markedly decreased (Figure 1I), which has been speculated to be a cause of NK.[13] These results indicate the potential roles of corneal nerves and the released SP in the regulation of LSCs.

SP enhances the proliferation and stemness of LSCs *in vitro*

To explore the roles of exogenous SP in regulating LSCs functions, the LSCs were cultured with SHEM containing different concentrations of SP for 5 days. Comparing with the control group, the outgrowth area of LSCs explants treated with SP was larger (Figures 2A and 2B), which indicated that SP promoted the proliferation of LSCs. Subsequently, the LSC-positive marker DeltaNp63[31] and proliferation marker Ki67 were stained. We found that LSCs incubated with 1 and 5 μM SP expressed higher levels of DeltaNp63 and Ki67 than that of control group (Figure 2C). These results indicated that exogenous SP not only enhanced proliferation but also the stemness of LSCs *in vitro*.

SP rescues corneal defects, sensitivity, and stemness of LSCs *in vivo*

To verify the roles of SP in LSCs *in vivo*, we constructed a mouse NK model with or without topical SP application for 3 days. Corneal fluorescein sodium staining showed that NK caused corneal defects, whereas topical SP application partially rescued the defects (Figure 3A). Moreover, corneal denervation led to attenuation of corneal sensitivity. But the topical application of SP to denervated mice rescued the decreased corneal sensitivity (Figure 3B). In addition, the downregulation of LSCs markers, *p63* and *Abcg2*, was also partially recovered (Figure 3C). The results suggested that topical SP application promoted the repairment of corneal epithelium, recovery of corneal sensitivity, and partially recovered the stemness of LSCs *in vivo*.

Subconjunctival injection of NK1R antagonist causes similar pathological changes as in corneal denervated mice

SP mainly functions by binding to the NK1R.[32] To explore the effects of blocking the SP-NK1R pathway on mouse corneas, we subconjunctivally injected the NK1R antagonist L-733,060 twice in wild-type mice.

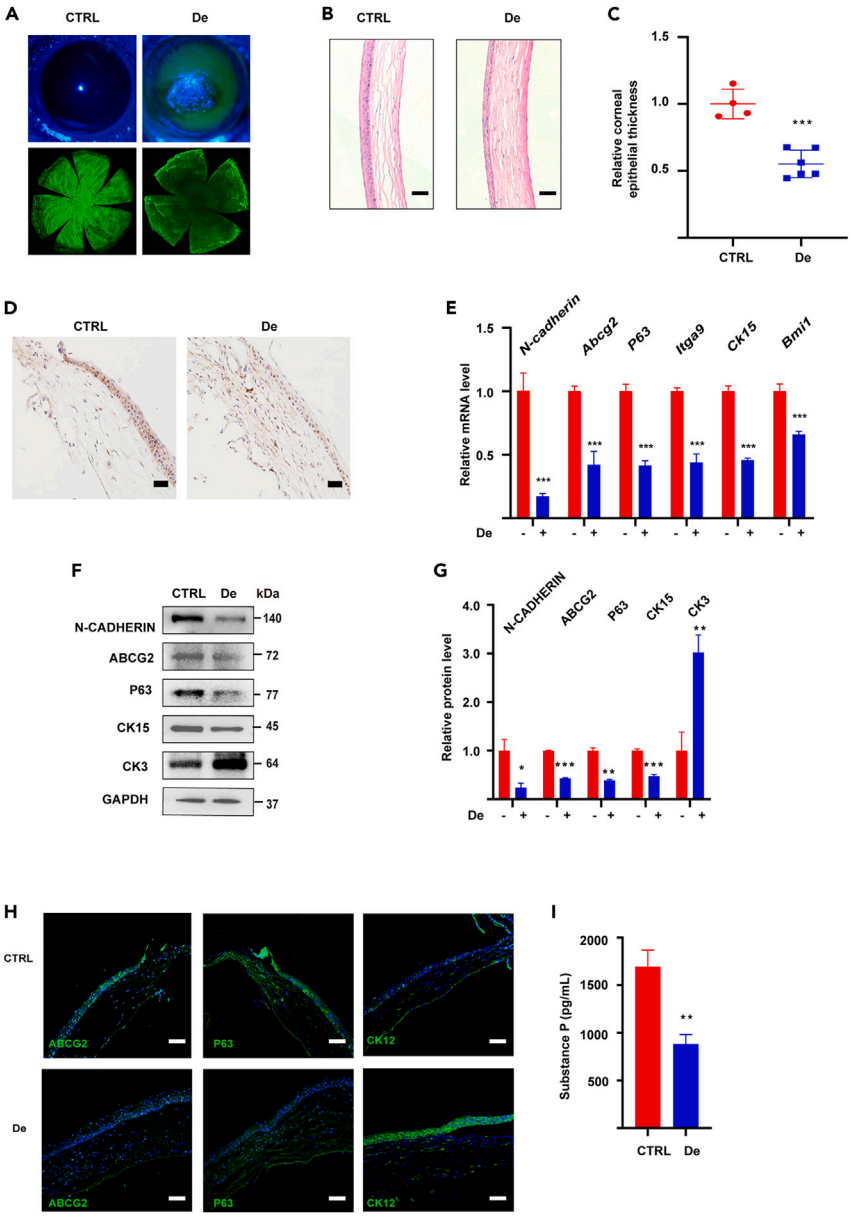

Figure 1. Corneal denervation reduces SP level

(A) After 1 week of corneal denervation in normal mice, corneal epithelial defects and nerve degeneration were detected with fluorescein sodium staining and whole-mount corneal staining. CTRL: control; De: denervation. n = 4 per group.

(B and C) HE staining of corneas of control and denervated mice was performed to identify the corneal epithelial thickness (B). Quantification of the corneal epithelial thickness (C). n = 4 for control mice, and n = 6 for denervated mice. Scale bar: 20 μm.

(D) Immunohistochemistry staining for proliferation marker Ki67 was performed in the limbal region of control and denervated mice. n = 3 per group. Scale bar: 100 μm.

(E and F) The levels of LSC-positive markers and epithelial cell marker in limbal tissues after corneal denervation treatment as determined by qRT-PCR (E) and Western blot (F).

(G) The densitometric quantification of Western blot results. GAPDH was used as control.

(H) *In situ* RNA hybridization of LSC-positive markers and epithelial cell marker on limbal region of normal and denervated mice. Scale bar: 200 μm.

(I) ELISA showing SP levels in corneas from normal and denervated mice. Data are presented as mean ± SEM. *$p < 0.05$, **$p < 0.01$, ***$p < 0.001$.

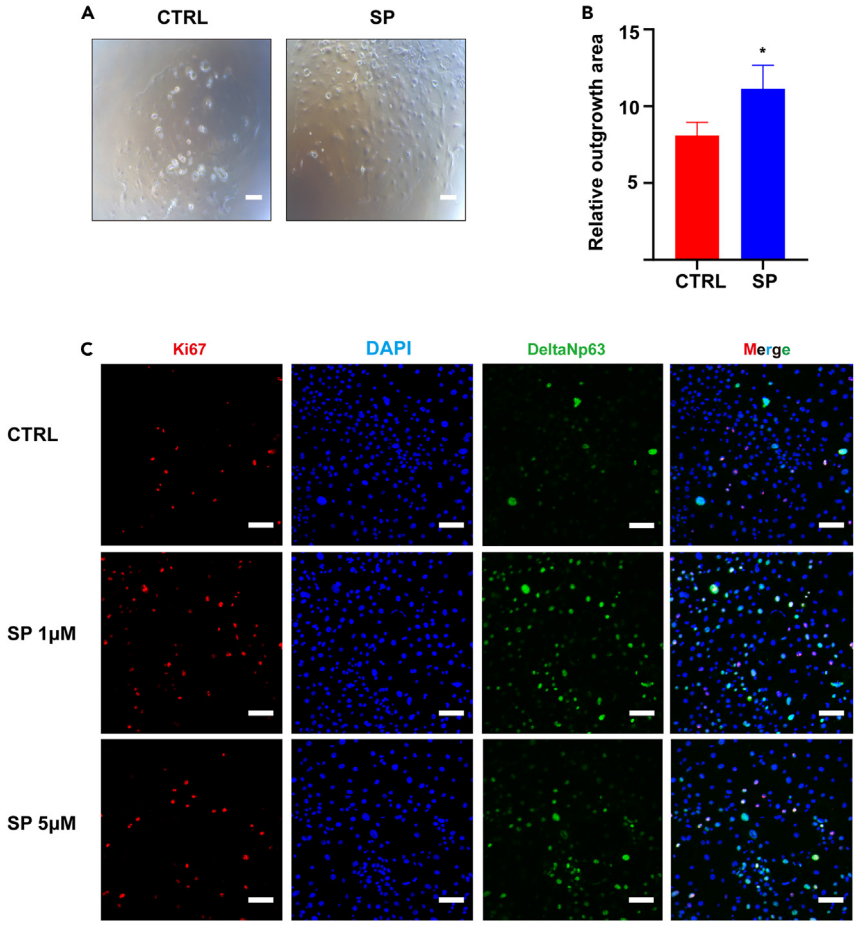

Figure 2. SP enhances the proliferation and stemness of LSCs *in vitro*

(A) Images of LSCs explants treated with or without SP (5 μM) at day 5, scale bar: 200 μm.

(B) Quantification of the relative outgrowth area of LSCs explants treated with or without SP (5 μM), n = 3 per group.

(C) Images of limbal stem cells stained with nuclear marker DAPI (blue), proliferation marker Ki67 (red), and LSCs marker DeltaNp63 (green) after treatment with or without SP (1 and 5 μM) for 5 days, scale bar: 500 μm. Data are presented as mean ± SEM. *$p < 0.05$.

Fluorescein sodium staining showed that the antagonist injection caused obvious corneal defects similar to those in the NK model mice (Figure 4A). Compared with control mice, corneal sensitivity decreased in injected mice (Figure 4B), accompanied by attenuated corneal epithelial thickness (Figures 4C and 4D). These pathological changes were similar to those observed in denervated mice. Immunohistochemistry staining showed that the expression of proliferation marker Ki67 was decreased in the limbus of antagonist-injected mice (Figure 4E). The result reflected that antagonist L-733,060 treatment weakened the proliferation of LSCs. In addition, LSC-positive markers levels were also downregulated; conversely, CK3, the corneal epithelial cell marker level, was upregulated in antagonist-injected mice limbal tissues (Figures 4F–4H). *In situ* hybridization was performed on normal and antagonist-injected mice limbus. It showed that the expression of ABCG2, P63 transcripts on limbal region was decreased in antagonist-injected mice. On the contrary, the level of the corneal epithelial cell marker, CK12, was increased (Figure 4I). The results suggested that LSCs stemness was similarly attenuated by subconjunctival injection of the antagonist. These data showed that subconjunctival injection of an NK1R antagonist caused similar pathological changes as in corneal denervated mice regarding corneal defects, sensitivity, epithelial thickness, proliferation, and attenuated LSCs stemness implying that the SP-NK1R pathway is vital for the repairment of corneal epithelium and the metabolism of LSCs.

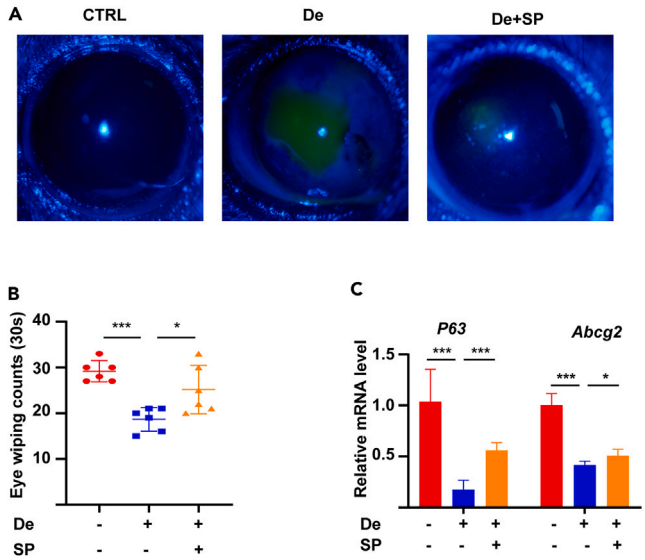

Figure 3. SP rescues corneal defects, sensitivity, and stemness of LSCs *in vivo*

(A) Corneal fluorescein sodium staining showing the corneal defects of the denervated mice with or without SP treatment. n = 6 per group.

(B) Eye-wiping counts in control, denervated mice, and denervated mice with SP treatment, reflecting the corneal sensitivity. n = 6 per group.

(C) qRT-PCR results showing that topical SP application partially recovered denervation-induced downregulation of LSCs markers *p63* and *Abcg2* in limbal tissues. Data are presented as mean ± SEM. *p < 0.05, ***p < 0.001.

PI3K-AKT signaling pathway mediates effects of SP on LSCs

To explore the pathway induced by SP-NK1R signaling in LSCs, we injected an NK1R antagonist subconjunctivally to block the effects of SP. We then performed RNA sequencing with limbal tissues of normal mice and antagonist-injected mice and filtered out 1927 upregulated and 1458 downregulated genes in limbal tissues of antagonist-injected mice (>2.0-fold change, *q*-value <0.05, Figure 5A). Gene Ontology analysis showed that the genes related to LSCs stemness and proliferation were downregulated in antagonist-injected group, such as *Abcg2*, *Ck5*, *Fzd7*, *Ck15*, *Cyclin A*, and *S100a6* (Figure 5B). In addition, numerous genes in the PI3K-AKT signaling pathway were downregulated by the local injection of the antagonist (Figure 5C), suggesting that important functions of the pathway may be regulated by SP-NK1R signaling. Consistently, western blot showed that antagonist injection reduced AKT phosphorylation (*p*-AKT) in the limbal tissues (Figures 5D and 5E). Interestingly, the level of phosphorylated AKT also decreased in denervated mouse limbal tissues (Figures 5F and 5G), which showed decreased SP level (Figure 1F). The results showed that blocking SP-NK1R signaling could repress the PI3K-AKT pathway in the mouse limbus, indicating that SP may regulate LSCs functions through PI3K-AKT signaling.

PI3K-AKT signaling pathway inhibitor attenuates the rescue effects of SP on LSCs

To explore the mechanism of the positive effects of SP on LSCs, an AKT inhibitor MK-2206 (1 μM) was applied to SP-treated LSCs for 5 days. As previously described, SP promoted the expression of proliferation marker Ki67 and LSC-positive marker DeltaNp63 (Figure 6A). However, MK-2206 treatment markedly attenuated the positive effects of SP on LSCs (Figure 6A). To verify the effects of blocking the PI3K-AKT signaling pathway on mouse corneas, we subconjunctivally injected the AKT inhibitor MK-2206 (10 μM) in wild-type mice. Fluorescein sodium staining showed that the AKT inhibitor injection caused obvious corneal defects similar to those in the NK model mice (Figure 6B). Immunohistochemistry staining showed that the expression of proliferation marker Ki67 was decreased in the limbus of AKT inhibitor-injected mice (Figure 6C). The result reflected that AKT inhibitor injection weakened the proliferation of LSCs. In addition, *in situ* hybridization was performed on mice limbus. It showed that the expression of ABCG2, P63 transcripts on limbal region was decreased and the level of CK12 was increased in AKT inhibitor-injected mice (Figure 6D). These results reflected that blocking AKT signaling pathway can attenuate the proliferation and stemness of LSCs *in vivo*. So, we suggested that SP-NK1R interaction modulates the PI3K-AKT signaling pathway to promote the proliferation and stemness of LSCs.

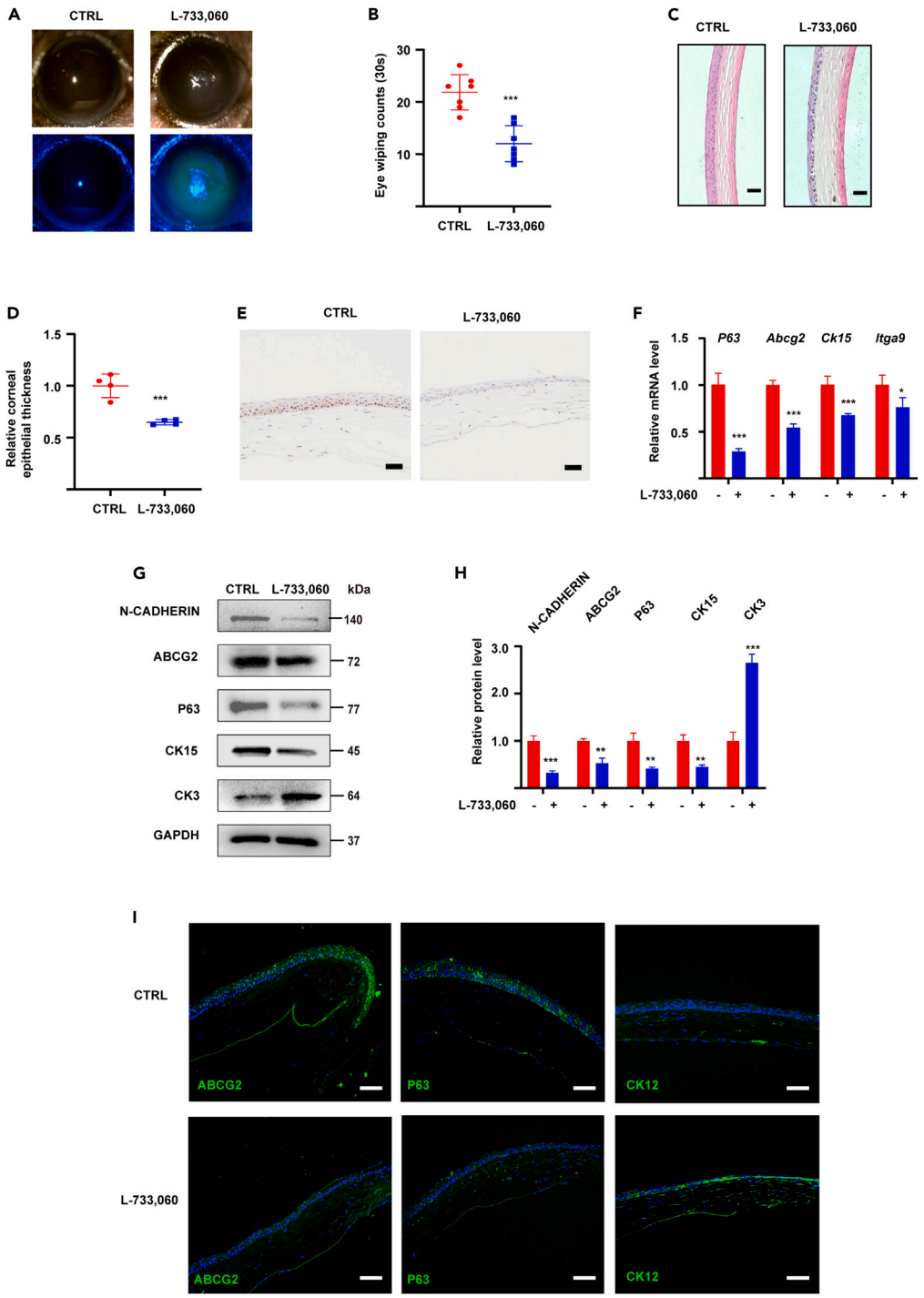

Figure 4. Subconjunctival injection of NK-1 receptor antagonist causes similar pathological changes as in corneal denervated mice

(A and B) Corneal fluorescein sodium staining and eye-wiping test results showing similar corneal changes (A) and attenuated corneal sensitivity (B) as in denervated mice after local injection of the antagonist. n = 6 per group.

(C and D) HE staining of corneas of control and antagonist-injected mice to identify the corneal epithelial thickness (C). Quantification of corneal epithelial thickness (D). n = 6 per group. Scale bar: 20 μm.

(E) Immunohistochemistry staining for proliferation marker Ki67 was performed in the limbal region of control and antagonist-injected mice. n = 3 per group. Scale bar: 100 μm.

Figure 4. *Continued*
(F and G) The levels of LSC-positive markers and epithelial cell marker in limbal tissues after local injection of the antagonist as determined by qRT-PCR (F) and Western blot (G).
(H) The densitometric quantification of Western blot results. GAPDH was used as control.
(I) *In situ* RNA hybridization of LSC-positive markers and epithelial cell marker on limbal region of normal and antagonist-injected mice. Scale bar: 200 μm. Data are presented as mean ± SEM. *p < 0.05, **p < 0.01, ***p < 0.001.

DISCUSSION

Uncontrolled dysfunction or deficiency of LSCs can result in devastating blindness-causing diseases. Therefore, tightly regulating the biological characteristics of LSCs is essential to prevent their dysfunction or the progression to blindness. However, the regulatory factors of LSCs and the underlying mechanisms are poorly understood. In this study, our findings showed that the trigeminal nerve participated in regulating the LSCs niche microenvironment, and the trigeminal nerve-derived SP was a potent regulating factor of LSCs in rescuing corneal defects, corneal sensitivity, and LSC-positive markers levels in denervated mice and promoted LSCs proliferation and stemness via the PI3K-AKT signaling pathway.

Previous studies have shown that topical SP-derived peptide FGLM-amide can be administered to patients with neurotrophic keratopathy, resulting in the closure of epithelial defects and amelioration of corneal opacity.[33,34] To date, the protective effects of SP on corneal homeostasis are poorly understood. Here, we found that topical application of SP rescued corneal defects and the expression of LSC-positive markers in a neurotrophic keratopathy mouse model, suggesting that SP may maintain the corneal homeostasis by promoting the biological characteristics of LSCs. In addition, SP markedly promoted the proliferation and stemness of LSCs *in vitro*, verifying the positive effects of SP on LSCs. Moreover, both $NK1R^{-/-}$ mice and NK1R antagonist-injected mice showed corneal epithelial defects, suggesting that SP is vital for maintaining corneal homeostasis.[15,35] Importantly, we found that injecting NK1R antagonist not only caused corneal defects but also decreased the expression of LSC-positive markers, verifying the role of SP in regulating LSCs functions and corneal homeostasis.

However, our findings on the protective effects of SP on LSCs and the homeostasis of ocular surface present different standpoints from another study on *Tac1* gene knockout mice, which reported the opposite roles of SP in a limbal stem cell deficiency (LSCD) mouse model by showing that corneal defects and LSCD are ameliorated in *Tac1* knockout corneas, compared with wild-type corneas.[36] Traditionally, SP is known for its double-edged role, either in maintaining corneal homeostasis or in promoting inflammation. SP adversely affects ocular surface inflammation by promoting the release and activation of pro-inflammatory cytokines and growth factors in infected corneas.[14,37] Previous studies have reported that SP abolishment or NK1R antagonists can modulate inflammation and inhibit the production of inflammatory cytokines in corneas.[38,39] NK1R antagonist treatment showed protective effects in corneal alkali burn and neovascularization through reducing corneal hemangiogenesis and leukocyte infiltration.[40] The study was performed on the prolonged pro-inflammatory LSCD model, in which extensive inflammatory cell infiltration was observed in corneas,[41] accelerating apoptosis and depletion of stem cells. Stem cells deficiency occurring in the setting of inflammation could induce excessive release of SP and therefore its inhibition by means of NK1R antagonists is beneficial. These findings suggest that the effects of SP on corneal homeostasis and LSCs might be multifaceted or context specific. It is not surprising that the Vitar et al. study found that SP/NK1R pathway blockade could ameliorate LSCD in the pro-inflammatory model.[36] Our study showed that SP promoted the proliferation and stemness of LSCs *in vitro*. In addition, previous studies have reported that the effects of SP on corneal wound healing and bone marrow stem cells are concentration- or time-dependent.[14,42] Therefore, based on current evidence, we speculated that SP had the similar effects on LSCs. SP may promote proliferation or stemness at low concentrations and in a short time, but induce -detrimental effects at high levels and prolonged exposure. Further studies are required to verify this.

To date, the signaling pathways induced by SP-NK1R interaction are not well understood. AKT signaling can be activated by SP-NK1R interaction to prevent the apoptosis of corneal epithelial cells.[43] However, whether SP-NK1R interaction in LSCs also regulates AKT signaling remains unclear. In our study, RNA-seq revealed that SP-NK1R interaction mainly modulated the PI3K-AKT signaling pathway in limbal tissues. In addition, the AKT pathway modulates the functional properties of LSCs.[44] We found that topical injection of an NK1R antagonist suppressed *p*-AKT and the expression of LSC-positive markers in limbal tissues.

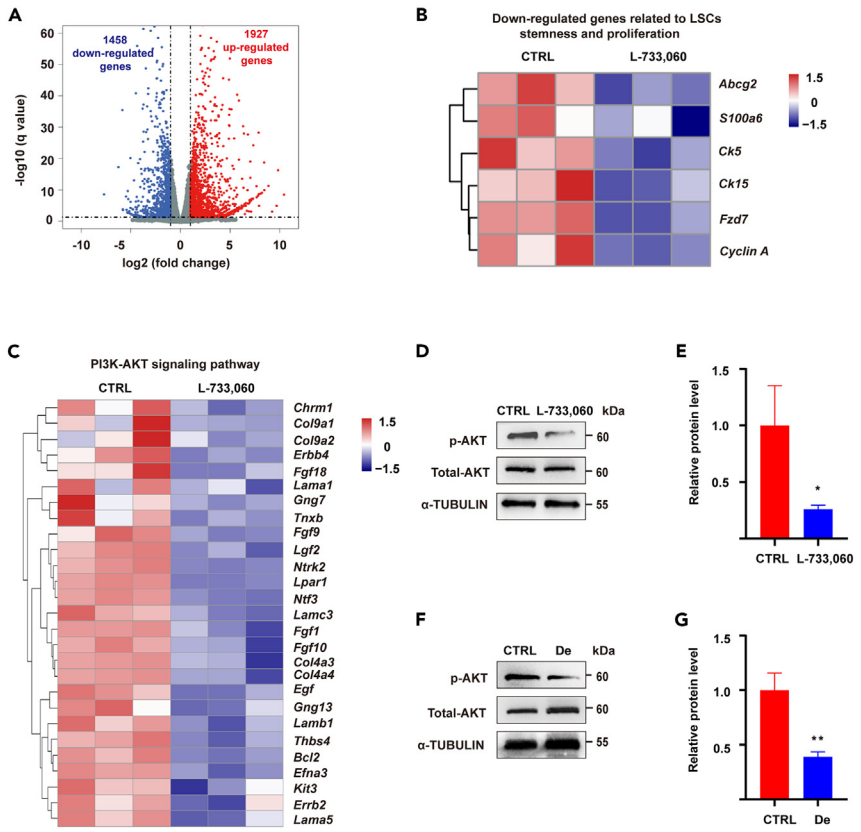

Figure 5. PI3K-AKT signaling pathway mediates the rescue effects of SP on LSCs

(A) A volcano plot of RNA-seq of control and antagonist-injected mice limbal tissues showing 1927 upregulated and 1458 downregulated genes (>2.0-fold change, *q*-value <0.05).

(B) Heatmap showing the LSCs stemness and proliferation related genes in control and antagonist-injected mice.

(C) Heatmap showing the differentially expressed genes related to PI3K-AKT signaling in control and antagonist-injected mice.

(D and F) Western blot results showing reduced AKT phosphorylation in limbal tissues of denervated (D) and antagonist-injected (F) mice.

(E and G) The densitometric quantification of Western blot results in limbal tissues of denervated (E) and antagonist-injected (G) mice. α-TUBULIN was used as control. Data are presented as mean ± SEM. *p < 0.05, **p < 0.01.

Furthermore, blocking the pathway in LSCs markedly reduced SP-induced promotion of proliferation and stemness, indicating that SP-NK1R interaction induced positive effects on LSCs by regulating the AKT signaling pathway and the downstream factors.

In summary, we demonstrated the positive effects of SP on the biological characteristics of LSCs both *in vivo* and *in vitro*. We revealed that SP regulates PI3K-AKT signaling to mediate its effects. Our study provides new insight about the role of SP in regulating corneal homeostasis and LSCs, suggesting the potential therapeutic implications of SP for LSCs transplantation for severe LSCD diseases.

Limitation of the study

Because SP played double-edged roles in the corneas, we speculated the positive effects of SP on LSCs, promoting proliferation or stemness at low concentrations and in a short time but inducing detrimental effects at high levels and prolonged exposure. We suggest further verification by varying SP concentrations and incubation time.

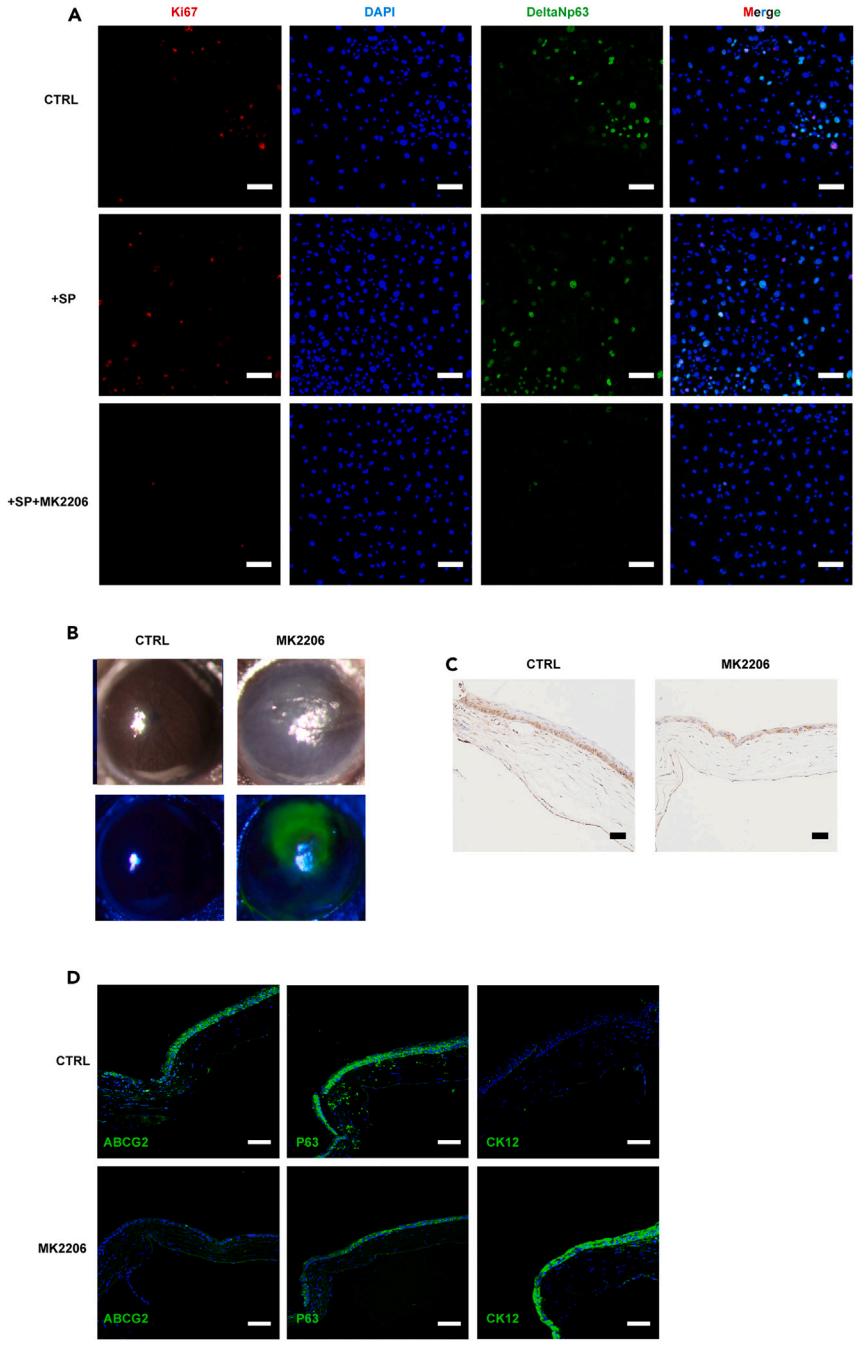

Figure 6. PI3K-AKT signaling pathway inhibitor attenuates SP effects on LSCs

(A) Images of SP-treated limbal stem cells stained with nuclear marker DAPI (blue), proliferation marker Ki67 (red), and LSCs marker DeltaNp63 (green) after AKT inhibitor MK-2206 (1 μM) was applied for 5 days. Scale bar: 500 μm.

(B) Corneal fluorescein sodium staining showing corneal defects after subconjunctival injection of AKT inhibitor MK-2206 (10 μM). n = 6 per group.

(C) Immunohistochemistry staining for proliferation marker Ki67 was performed in the limbal region of control and AKT inhibitor-injected mice. n = 3 per group. Scale bar: 100 μm.

(D) *In situ* RNA hybridization of LSC-positive markers and epithelial cell marker on limbal region of normal and AKT inhibitor-injected mice. Scale bar: 200 μm.

STAR★METHODS

Detailed methods are provided in the online version of this paper and include the following:

- KEY RESOURCES TABLE
- RESOURCE AVAILABILITY
  - Lead contact
  - Materials availability
  - Data and code availability
- EXPERIMENTAL MODEL AND SUBJECT DETAILS
  - *In vivo* mouse corneal denervation model and treatment
- METHOD DETAILS
  - Subconjunctival injection
  - Whole-mount corneal staining
  - Eye-wiping test
  - Cells culture and treatment
  - Substance P ELISA
  - Western blot analysis
  - Immunofluorescence staining
  - Immunohistochemical staining
  - *In situ* hybridization (ISH)
  - Quantitative real-time PCR (qRT-PCR)
  - RNA sequencing (RNA-seq)
- QUANTIFICATION AND STATISTICAL ANALYSIS

ACKNOWLEDGMENTS

We would like to thank Editage (www.editage.cn) for English language editing. This study was funded by the National Natural Science Foundation of China (81870631).

AUTHOR CONTRIBUTIONS

S.W., Z.W., and P.X. conceived and designed the study, P.X., X.L., X.D., and Y.L. performed experiments, P.X. analyzed the data and wrote the manuscript, S.W. and Z.W. revised the manuscript.

DECLARATION OF INTERESTS

The authors declare no competing interests.

INCLUSION AND DIVERSITY

We support inclusive, diverse, and equitable conduct of research.

Received: October 3, 2022
Revised: March 4, 2023
Accepted: April 13, 2023
Published: April 18, 2023

REFERENCES

1. Yazdanpanah, G., Jabbehdari, S., and Djalilian, A.R. (2017). Limbal and corneal epithelial homeostasis. Curr. Opin. Ophthalmol. *28*, 348–354. https://doi.org/10.1097/icu.0000000000000378.

2. Bonnet, C., González, S., Roberts, J.S., Robertson, S.Y.T., Ruiz, M., Zheng, J., and Deng, S.X. (2021). Human limbal epithelial stem cell regulation, bioengineering and function. Prog. Retin. Eye Res. *85*, 100956. https://doi.org/10.1016/j.preteyeres.2021.100956.

3. Pellegrini, G., Rama, P., Di Rocco, A., Panaras, A., and De Luca, M. (2014). Concise review: hurdles in a successful example of limbal stem cell-based regenerative medicine. Stem Cell. *32*, 26–34. https://doi.org/10.1002/stem.1517.

4. Peterson, S.C., Eberl, M., Vagnozzi, A.N., Belkadi, A., Veniaminova, N.A., Verhaegen, M.E., Bichakjian, C.K., Ward, N.L., Dlugosz, A.A., and Wong, S.Y. (2015). Basal cell carcinoma preferentially arises from stem cells within hair follicle and mechanosensory niches. Cell Stem Cell *16*, 400–412. https://doi.org/10.1016/j.stem.2015.02.006.

5. Ameku, T., Yoshinari, Y., Texada, M.J., Kondo, S., Amezawa, K., Yoshizaki, G., Shimada-Niwa, Y., and Niwa, R. (2018). Midgut-derived neuropeptide F controls germline stem cell proliferation in a mating-dependent manner. PLoS Biol. *16*, e2005004. https://doi.org/10.1371/journal.pbio.2005004.

6. Aerts-Kaya, F., Ulum, B., Mammadova, A., Köse, S., Aydin, G., Korkusuz, P., and Uçkan-Çetinkaya, D. (2020). Neurological regulation of the. Adv. Exp. Med. Biol. *1212*, 127–153. https://doi.org/10.1007/5584_2019_398.

7. Knox, S.M., Lombaert, I.M.A., Haddox, C.L., Abrams, S.R., Cotrim, A., Wilson, A.J., and

Hoffman, M.P. (2013). Parasympathetic stimulation improves epithelial organ regeneration. Nat. Commun. *4*, 1494. https://doi.org/10.1038/ncomms2493.

8. Eguchi, H., Hiura, A., Nakagawa, H., Kusaka, S., and Shimomura, Y. (2017). Corneal nerve fiber structure, its role in corneal function, and its changes in corneal diseases. Preprint at bioRxiv. https://doi.org/10.1155/2017/3242649.

9. Müller, L.J., Marfurt, C.F., Kruse, F., and Tervo, T.M.T. (2003). Corneal nerves: structure, contents and function. Exp. Eye Res. *76*, 521–542. https://doi.org/10.1016/s0014-4835(03)00050-2.

10. Al-Aqaba, M., Dhillon, V.K., Mohammed, I., Said, D.G., and Dua, H.S. (2019). Corneal nerves in health and disease. Prog. Retin. Eye Res. *73*, 100762. https://doi.org/10.1016/j.preteyeres.2019.05.003.

11. Ueno, H., Ferrari, G., Hattori, T., Saban, D.R., Katikireddy, K.R., Chauhan, S.K., and Dana, R. (2012). Dependence of corneal stem/progenitor cells on ocular surface innervation. Invest. Ophthalmol. Vis. Sci. *53*, 867–872. https://doi.org/10.1167/iovs.11-8438.

12. Hsu, H.Y., and Modi, D. (2015). Etiologies, quantitative hypoesthesia. Eye Contact Lens *41*, 314–317. https://doi.org/10.1097/icl.0000000000000133.

13. Goins, K.M. (2005). New insights into the diagnosis and treatment of neurotrophic keratopathy. Ocul. Surf. *3*, 96–110. https://doi.org/10.1016/s1542-0124(12)70158-1.

14. Singh, R.B., Naderi, A., Cho, W., Ortiz, G., Musayeva, A., Dohlman, T.H., Chen, Y., Ferrari, G., and Dana, R. (2022). Modulating the tachykinin: role of substance P and neurokinin receptor expression in ocular surface disorders. Ocul. Surf. *25*, 142–153. https://doi.org/10.1016/j.jtos.2022.06.007.

15. Yang, L., Di, G., Qi, X., Qu, M., Wang, Y., Duan, H., Danielson, P., Xie, L., and Zhou, Q. (2014). Substance P promotes diabetic corneal epithelial wound healing through molecular mechanisms mediated via the neurokinin-1 receptor. Diabetes *63*, 4262–4274. https://doi.org/10.2337/db14-0163.

16. Nakamura, M., Nagano, T., Chikama, T., Nishida, T., and communications, b.r. (1998). Up-regulation of phosphorylation of focal adhesion kinase and paxillin by combination of substance P and IGF-1 in SV-40 transformed human corneal epithelial cells. Biochem. Biophys. Res. Commun. *242*, 16–20. https://doi.org/10.1006/bbrc.1997.7899.

17. Ma, D.H.K., Chen, H.C., Ma, K.S.K., Lai, J.Y., Yang, U., Yeh, L.K., Hsueh, Y.J., Chu, W.K., Lai, C.H., and Chen, J.K. (2016). Preservation of human limbal epithelial progenitor cells on carbodiimide cross-linked amniotic membrane via integrin-linked kinase-mediated Wnt activation. Acta Biomater. *31*, 144–155. https://doi.org/10.1016/j.actbio.2015.11.042.

18. Ko, J.A., Mizuno, Y., Ohki, C., Chikama, T.i., Sonoda, K.H., Kiuchi, Y., and science, v. (2014). Neuropeptides released from trigeminal neurons promote the stratification of human corneal epithelial cells. Invest. Ophthalmol. Vis. Sci. *55*, 125–133. https://doi.org/10.1167/iovs.13-12642.

19. Polisetti, N., Zenkel, M., Menzel-Severing, J., Kruse, F.E., and Schlötzer-Schrehardt, U. (2016). Cell adhesion molecules and stem cell-niche-interactions in the limbal stem cell niche. Stem Cell. *34*, 203–219. https://doi.org/10.1002/stem.2191.

20. Calautti, E. (2013). Akt modes of stem cell regulation: more than meets the eye? Discoveries *1*, e8. https://doi.org/10.15190/d.2013.8.

21. Yamaguchi, T., Turhan, A., Harris, D.L., Hu, K., Prüss, H., von Andrian, U., and Hamrah, P. (2013). Bilateral nerve alterations in a unilateral experimental neurotrophic keratopathy model: a lateral conjunctival approach for trigeminal axotomy. PLoS One *8*, e70908. https://doi.org/10.1371/journal.pone.0070908.

22. Hayashi, R., Yamato, M., Sugiyama, H., Sumide, T., Yang, J., Okano, T., Tano, Y., and Nishida, K. (2007). N-Cadherin is expressed by putative stem/progenitor cells and melanocytes in the human limbal epithelial stem cell niche. Stem Cell. *25*, 289–296. https://doi.org/10.1634/stemcells.2006-0167.

23. Budak, M.T., Alpdogan, O.S., Zhou, M., Lavker, R.M., Akinci, M.A.M., and Wolosin, J.M. (2005). Ocular surface epithelia contain ABCG2-dependent side population cells exhibiting features associated with stem cells. J. Cell Sci. *118*, 1715–1724. https://doi.org/10.1242/jcs.02279.

24. Umemoto, T., Yamato, M., Nishida, K., Yang, J., Tano, Y., and Okano, T. (2006). Limbal epithelial side-population cells have stem cell-like properties, including quiescent state. Stem Cell. *24*, 86–94. https://doi.org/10.1634/stemcells.2005-0064.

25. Kawakita, T., Shimmura, S., Higa, K., Espana, E.M., He, H., Shimazaki, J., Tsubota, K., Tseng, S.C.G., and science, v. (2009). Greater growth potential of p63-positive epithelial cell clusters maintained in human limbal epithelial sheets. Invest. Ophthalmol. Vis. Sci. *50*, 4611–4617. https://doi.org/10.1167/iovs.08-2586.

26. Pajoohesh-Ganji, A., Pal-Ghosh, S., Simmens, S.J., and Stepp, M.A. (2006). Integrins in slow-cycling corneal epithelial cells at the limbus in the mouse. Stem Cell. *24*, 1075–1086. https://doi.org/10.1634/stemcells.2005-0382.

27. Yoshida, S., Shimmura, S., Kawakita, T., Miyashita, H., Den, S., Shimazaki, J., Tsubota, K., and science, v. (2006). Cytokeratin 15 can be used to identify the limbal phenotype in normal and diseased ocular surfaces. Invest. Ophthalmol. Vis. Sci. *47*, 4780–4786. https://doi.org/10.1167/iovs.06-0574.

28. Joe, A., and Yeung, S.N. (2014). Concise review: identifying limbal stem cells: classical concepts and new challenges. Stem Cells Translational Medicine *3*, 318–322. https://doi.org/10.5966/sctm.2013-0137.

29. Schermer, A., Galvin, S., and Sun, T.T. (1986). Differentiation-related expression of a major 64K corneal keratin in vivo and in culture suggests limbal location of corneal epithelial stem cells. J. Cell Biol. *103*, 49–62. https://doi.org/10.1083/jcb.103.1.49.

30. Kawasaki, S., Tanioka, H., Yamasaki, K., Yokoi, N., Komuro, A., Kinoshita, S., and science, v. (2006). Clusters of corneal epithelial cells reside ectopically in human conjunctival epithelium. Invest. Ophthalmol. Vis. Sci. *47*, 1359–1367. https://doi.org/10.1167/iovs.05-1084.

31. Di Iorio, E., Barbaro, V., Ruzza, A., Ponzin, D., Pellegrini, G., and De Luca, M. (2005). Isoforms of DeltaNp63 and the migration of ocular limbal cells in human corneal regeneration. Proc. Natl. Acad. Sci. USA *102*, 9523–9528. https://doi.org/10.1073/pnas.0503437102.

32. Mantyh, P.W. (2002). Neurobiology of Substance P and the NK1 Receptor. J. Clin. Psychiatry *63*, 6–10.

33. Chikama, T., Fukuda, K., Morishige, N., and Nishida, T. (1998). Treatment of neurotrophic keratopathy with substance-P-derived peptide (FGLM) and insulin-like growth factor I. Lancet *351*, 1783–1784. https://doi.org/10.1016/s0140-6736.

34. Yanai, R., Nishida, T., Chikama, T., Morishige, N., Yamada, N., and Sonoda, K.J.C. (2015). Potential new modes of treatment of neurotrophic keratopathy. Cornea *34*, S121–S127. https://doi.org/10.1097/ico.0000000000000587.

35. Gaddipati, S., Rao, P., Jerome, A.D., Burugula, B.B., Gerard, N.P., and Suvas, S. (2016). Loss of neurokinin-1 receptor alters ocular surface homeostasis and promotes an early development of herpes stromal keratitis. J. Immunol. *197*, 4021–4033. https://doi.org/10.4049/jimmunol.1600836.

36. Lasagni Vitar, R., Triani, F., Barbariga, M., Fonteyne, P., Rama, P., and Ferrari, G. (2022). Substance P/neurokinin-1 receptor pathway blockade ameliorates limbal stem cell deficiency by modulating mTOR pathway and preventing cell senescence. Stem Cell Rep. *17*, 849–863. https://doi.org/10.1016/j.stemcr.2022.02.012.

37. Suvas, S. (2017). Role of substance P neuropeptide in inflammation, wound healing, and tissue homeostasis. J. Immunol. *199*, 1543–1552. https://doi.org/10.4049/jimmunol.1601751.

38. Barbariga, M., Fonteyne, P., Ostadreza, M., Bignami, F., Rama, P., Ferrari, G., and science, v. (2018). Substance P modulation of human and murine corneal neovascularization. Invest. Ophthalmol. Vis. Sci. *59*, 1305–1312. https://doi.org/10.1167/iovs.17-23198.

39. Lucas, K., Karamichos, D., Mathew, R., Zieske, J.D., and Stein-Streilein, J. (2012). Retinal laser burn-induced neuropathy leads to substance P-dependent loss of ocular immune privilege. J. Immunol. *189*, 1237–1242. https://doi.org/10.4049/jimmunol.1103264.

40. Bignami, F., Giacomini, C., Lorusso, A., Aramini, A., Rama, P., Ferrari, G., and science, v. (2014). NK1 receptor antagonists as a new treatment for corneal neovascularization. Invest. Ophthalmol. Vis. Sci. *55*, 6783–6794. https://doi.org/10.1167/iovs.14-14553.

41. Kethiri, A.R., Raju, E., Bokara, K.K., Mishra, D.K., Basu, S., Rao, C.M., Sangwan, V.S., and Singh, V. (2019). Inflammation, vascularization and goblet cell differences in LSCD: validating animal models of corneal alkali burns. Exp. Eye Res. *185*, 107665. https://doi.org/10.1016/j.exer.2019.05.005.

42. Nowicki, M., Ostalska-Nowicka, D., Kondraciuk, B., and Miskowiak, B. (2007). The significance of substance P in physiological and malignant haematopoiesis. J. Clin. Pathol. *60*, 749–755. https://doi.org/10.1136/jcp.2006.041475.

43. Yang, L., Sui, W., Li, Y., Qi, X., Wang, Y., Zhou, Q., and Gao, H. (2016). Substance P inhibits hyperosmotic stress-induced apoptosis in corneal epithelial cells through the mechanism of akt activation and reactive oxygen species scavenging via the neurokinin-1 receptor. PLoS One *11*, e0149865. https://doi.org/10.1371/journal.pone.0149865.

44. Saoncella, S., Tassone, B., Deklic, E., Avolio, F., Jon, C., Tornillo, G., De Luca, E., Di Iorio, E., Piva, R., Cabodi, S., et al. (2014). Nuclear Akt2 opposes limbal keratinocyte stem cell self-renewal by repressing a FOXO-mTORC1 signaling pathway. Stem Cell. *32*, 754–769. https://doi.org/10.1002/stem.1565.

45. Marco, B., Alessandro, R., Philippe, F., Fabio, B., Paolo, R., Giulio, F., and science, v. (2018). The effect of aging on nerve morphology and substance P expression in mouse and human corneas. Invest. Ophthalmol. Vis. Sci. *59*, 5329–5335. https://doi.org/10.1167/iovs.18-24707.

46. Hou, L., Fu, W., Liu, Y., Wang, Q., Wang, L., Huang, Y., and science, v. (2020). Agrin promotes limbal stem cell proliferation and corneal wound healing through hippo-yap signaling pathway. Invest. Ophthalmol. Vis. Sci. *61*, 7. https://doi.org/10.1167/iovs.61.5.7.

STAR★METHODS

KEY RESOURCES TABLE

REAGENT or RESOURCE	SOURCE	IDENTIFIER
Antibodies		
ABCG2 antibody	Abcam	Cat#ab130244; RRID:AB_11156755
β III-tubulin antibody	Abcam	Cat#ab18207; RRID:AB_444319
Cytokeratin 15 antibody	Abcam	Cat#ab52816; RRID:AB_869863
P63 antibody	Santa Cruz	Cat#sc-25268; RRID:AB_628092
cytokeratin 3 antibody	Millipore	Cat#CBL218; RRID:AB_93425
N-cadherin antibody	Cell Signaling Technology	Cat#13116T; RRID:AB_2687616
AKT (pan) antibody	Cell Signaling Technology	Cat#4691; RRID:AB_915783
Phospho-AKT antibody	Cell Signaling Technology	Cat#4060; RRID:AB_2315049
Ki67 antibody	Abcam	Cat#ab279653; RRID: AB_2934265
DeltaNp63 antibody	Abcam	Cat#ab203826; RRID:AB_2934266
α-tubulin antibody	Ray Antibody	Cat#RM2007; RRID:AB_2934267
GAPDH antibody	Fude Biological Technology	Cat#FD0063; RRID:AB_2934268
Goat anti-mouse IgG antibody	Fude Biological Technology	Cat#FDM007; RRID:AB_2934269
Goat anti-rabbit IgG antibody	Fude Biological Technology	Cat#FDR007; RRID:AB_2934270
Alexa Fluor-conjugated secondary antibodies	Thermo Fisher Scientific	Cat#A-11008; RRID:AB_143165
Chemicals, peptides, and recombinant proteins		
Substance P	MedChemExpress	Cat # HY-P0201
L-733,060	TOCRIS	Cat#1145
Zamboni fixative solution	Solarbio	Cat#G2190
Dispase II	Sigma-Aldrich	Cat#D4693
DMEM/F12 medium	Corning Life Sciences	Cat#10-092-CVRC
FBS	Gibco	Cat#10099-141
Insulin	Sigma-Aldrich	Cat#I2643
Transferrin	Sigma-Aldrich	Cat#T3309
Selenium	Sigma-Aldrich	Cat#S9133
Hydrocortisone	MedChemExpress	Cat#HY-N0583
Mouse epidermal growth factor	R&D Systems	Cat#2028-EG-200
Toxin A	Sigma-Aldrich	Cat#C8052
Gentamicin	Sigma-Aldrich	Cat#G1914
Amphotericin B	Sigma-Aldrich	Cat#V900919
Dimethyl sulfoxide	Sigma-Aldrich	Cat#D2650
MK-2206	MedChemExpress	Cat#HY-10358
Protease inhibitor	Beyotime Biotechnology	Cat#P1006
RIPA lysis buffer	Solarbio	Cat#R0020
PVDF membrane	Bio-Rad	Cat#1620219
DAPI	Fude Biological Technology	Cat#FD9637
TRIzol reagent	Thermo Fisher Scientific	Cat#15596-026
Critical commercial assays		
BCA Protein Assay Kit	Beyotime Biotechnology	Cat#P0009
SP ELISA kit	R&D Systems	Cat#KGE007

(*Continued on next page*)

Continued

REAGENT or RESOURCE	SOURCE	IDENTIFIER
FastKing RT Kit	TIANGEN	Cat#KR116
DAB kit	Maxim Biotech	Cat#DAB-0031
SYBR qPCR Master Mix	Vazyme Biotech	Cat#Q311-02
Biotin-labeled anti-digoxigenin antibody	BOSTER Biological Technology	Cat# Cat#AR0147
HRP Conjugated Streptavidin	BOSTER Biological Technology	BA1088
TSA reagents	PINUOFEI Biological Technology	Cat# PN1004, PN1006
Deposited data		
RNA-seq data	GEO database	GSE213140
Experimental models: Cell lines		
Mouse primary limbal stem cells	This paper	N/A
Experimental models: Organisms/strains		
C57BL/6 mice	Guangdong GemPharmatech Co., Ltd	Male and female, 6–8 weeks
Oligonucleotides		
Primer: *Gapdh* Forward: AGGTCGGTGTGAACGGATTTG Revers: TGTAGACCATGTAGTTGAGGTCA	This paper	N/A
Primer: *N-cadherin* Forward: AGCGCAGTCTTACCGAAGG Reverse: TCGCTGCTTTCATACTGAACTTT	This paper	N/A
Primer: *Abcg2* Forward: GAACTCCAGAGCCGTTAGGAC Revers: CAGAATAGCATTAAGGCCAGGTT	This paper	N/A
Primer: *P63* Forward: TACTGCCCCGACCCTTACAT Reverse: GCTGAGGAACTCGCTTGTCTG	This paper	N/A
Primer: *Itga9* Forward: CTGGAGCACTTCCACGACAAC Reverse: GGGTTGGTATGGACACGACA	This paper	N/A
Primer: *Ck15* Forward: AGCTATTGCAGAGAAAAACCGT Reverse: GGTCCGTCTCAGGTCTGTG	This paper	N/A
Primer: *Bmi-1* Forward: ATCCCCACTTAATGTGTGTCCT Reverse: CTTGCTGGTCTCCAAGTAACG	This paper	N/A
ISH probe for *Abcg2*: GCGAUUGUCAUGAGAAGUGUUGCUA	This paper	N/A
ISH probe for *P63*: AUGGUUAGGGCAUCGUUUCACAACC	This paper	N/A
ISH probe for *Ck12*: UGCUCCGUGUUGCUGCUGAUCUCUU	This paper	N/A
Software and algorithms		
GraphPad Prism 8	Graph Pad	N/A

RESOURCE AVAILABILITY

Lead contact

Further information and requests for resources should be directed to and will be fulfilled by the lead contact, Shuangyong Wang (364853063@qq.com).

Materials availability

All reagents were purchased commercially. This study did not generate new unique reagents.

Data and code availability

- RNA-seq data have been deposited at GEO database and are publicly available as of the date of publication. The accession number is listed in the key resources table.
- This paper does not report original code.
- Any additional information required to reanalyze the data reported in this paper is available from the lead contact upon request.

EXPERIMENTAL MODEL AND SUBJECT DETAILS

In vivo mouse corneal denervation model and treatment

All animal experiments were reviewed and approved by the Animal Care and Use Committee of the Third Affiliated Hospital of Guangzhou Medical University. The corneal denervation model was constructed as previously described.[21] C57BL/6J mice (6–8-week old) were systemically anesthetized with 4% chloral hydrate (10 mL/kg, intraperitoneally) and topically anesthetized with procainamide on the corneas. After cutting the temporal conjunctiva, the ciliary nerves, branch of the trigeminal nerves, were exposed and disconnected by microscopic tweezers. One week after surgery, an eye-wiping test and fluorescein sodium staining were performed. The corneal defects were visualized and photographed by a slit lamp (TOPCON, Tokyo, Japan). For topical SP application, 5 μL SP (1 mM, Cat # HY-P0201, MedChemExpress) was dropped on the corneal surface of each eye six times daily for 3 days after the corneal denervation experiment.[15]

METHOD DETAILS

Subconjunctival injection

For the subconjunctival injection, the NK1R antagonist L-733,060 (10 mg/mL, Cat#1145, TOCRIS) and AKT inhibitor MK-2206 (10 μM) was injected subconjunctivally twice on day 0 and 3. Meanwhile, sterile water were injected into control mice eyes.

Whole-mount corneal staining

Mouse eyes were enucleated and fixed in Zamboni fixative solution (Cat#G2190, Solarbio) for 30 min. The corneas were fixed for an additional hour and cut into petals. Then, the samples were permeabilized and blocked in 0.2% Triton X-100, 2% goat serum in 1× PBS for 2 h at room temperature followed by the incubation with anti-β III-tubulin primary antibody (1:100, Cat#ab18207, Abcam) at 4°C overnight and Alexa Fluor-conjugated secondary antibodies (1:500, Cat#A-11008, Thermo Fisher Scientific) for 1 h at room temperature. All images were captured using a laser scanning confocal microscope-LSM 880 with Airyscan (ZEISS, Oberkochen, Germany).

Eye-wiping test

The eye-wiping test is to assess mouse corneal nociception, which was performed as previously described.[45] Briefly, 10 μL NaCl solution (5 M) was dropped on the corneal surface of each eye followed by counting the eye-wiping with the forepaws for 30 s. The eye-wiping test can reflect corneal sensitivity.

Cells culture and treatment

Primary LSCs were isolated and cultured as previously described.[46] Briefly, the mouse eyeballs were extracted and washed three times with 1× PBS. Corneal and corneoscleral tissues were removed and digested in 2.4 U/mL Dispase II (Cat#D4693, Sigma-Aldrich) at 4°C overnight. The central cornea and iris tissues were removed. Then, the epithelial layer of the limbus was avulsed mechanically and cut into 12 equal pieces, which were laid on the bottom of a six-well plate. The cells were cultured with supplemental hormonal epithelial medium (SHEM) containing DMEM/F12 medium (Cat#10-092-CVRC, Corning Life Sciences) supplemented with 5% FBS (Cat#10099-141, Gibco), 5 μg/mL insulin (Cat#I2643, Sigma-Aldrich), 5 μg/mL transferrin (Cat#T3309, Sigma-Aldrich), 5 ng/mL selenium (Cat#S9133, Sigma-Aldrich), 0.5 μg/mL hydrocortisone (Cat#HY-N0583, MedChemExpress), 2 ng/mL mouse epidermal growth factor (Cat#2028-EG-200, R&D Systems), 30 ng/mL toxin A (Cat#C8052, Sigma-Aldrich), 50 μg/mL gentamicin (Cat#G1914, Sigma-Aldrich), 1.25 μg/mL amphotericin B (Cat#V900919, Sigma-Aldrich), and 0.5% dimethyl sulfoxide (Cat#D2650, Sigma-Aldrich).

For SP treatment, LSCs were treated with 1 μM or 5 μM SP for 5 days. For inhibitor treatment, the AKT inhibitor MK-2206 (1 μM, Cat#HY-10358, MedChemExpress) was applied to cells treated with SP for 5 days. The cells were then fixed for immunofluorescence staining.

Substance P ELISA

Each mouse cornea was placed in 100 μL of PBS containing 1% protease inhibitor (Cat#P1006, Beyotime Biotechnology). Samples from each group were in triplicate. All samples were homogenized using a homogenizer and centrifuged at 10,000 × g for 15 min at 4°C to collect the supernatants. Then, the levels of SP were quantitated using an SP ELISA kit (Cat#KGE007, R&D Systems) following the manufacturer's instructions.

Western blot analysis

Mouse limbal tissues were homogenized in RIPA lysis buffer (Cat#R0020, Solarbio) and lysed on ice for 20 min. Next, the lysates were quantitated using a BCA Protein Assay Kit (Cat#P0009, Beyotime Biotechnology). Approximately 15–30 μg protein samples were separated on an SDS-PAGE gel and transferred to a PVDF membrane (Cat#1620219, Bio-Rad), which was then blocked with 5% non-fat milk for 1 h at room temperature and incubated with the following antibodies at 4°C overnight: anti-ABCG2 (Cat#ab130244, Abcam), anti-cytokeratin 15 (CK15) (Cat#ab52816, Abcam), anti-P63 (Cat#sc-25268, Santa Cruz), anti-cytokeratin 3 (CK3) (Cat#CBL218, Millipore), anti-N-cadherin (Cat#13116T, CST), anti-AKT (Cat#4691, CST), anti-Phospho AKT (Cat#4060, CST), anti-α-tubulin (Cat#RM2007, Ray Antibody), anti-GAPDH (Cat#FD0063, Fude Biological Technology), goat anti-mouse IgG (Cat#FDM007, Fude Biological Technology), and goat anti-rabbit IgG (Cat#FDR007, Fude Biological Technology). The bands were detected using a ChemiDocTM Touch Imaging System (Bio-Rad).

Immunofluorescence staining

LSCs were cultured in six-well plates and treated with SP or AKT inhibitor MK-2206 for 5 days. The samples were then fixed with 4% paraformaldehyde and permeabilized with 0.1% Triton X-100 for 30 min followed by blocking using 5% goat serum for 30 min at room temperature. Incubation with the following antibodies was performed at 4°C overnight: anti-Ki67 (1:50, Cat#ab279653, Abcam) and anti-DeltaNp63 (1:50, Cat#ab203826, Abcam). Next, incubation with Alexa Fluor-conjugated secondary antibodies (1:500, Cat#A-21422/A-11008, Thermo Fisher Scientific) was carried out. The nuclei were stained using DAPI (Cat#FD9637, Fude Biological Technology). Finally, the cells were visualized using a laser scanning confocal microscope-LSM 880 with Airyscan (ZEISS, Oberkochen, Germany).

Immunohistochemical staining

The mouse corneas were harvested and fixed overnight in 4% paraformaldehyde solution at 4°C. The tissues were embedded in paraffin and cut into 5 μm thick sections, which were deparaffinized in xylene and ethanol. Subsequently, sections were incubated in 3% hydrogen peroxide for 10 min to block endogenous peroxidase activity, followed by heating the sections in citrate buffer (pH 6.0) for 10 min for antigen retrieval. The tissue sections were incubated with primary antibody Ki67 overnight at 4°C and then were incubated for 1 h at room temperature with goat anti-rabbit IgG. After washing with PBS three times for 10 min, the sections were stained with DAB substrate for 5–10 min. Finally, the sections were counterstained with hematoxylin for nuclear staining. Sections were captured using a fluorescence microscope-Axio Imager Z2 (ZEISS, Oberkochen, Germany).

In situ hybridization (ISH)

The corneas were fixed in 4% paraformaldehyde (PFA) solution for 24 h at 4°C. The fixed corneas were embedded in paraffin and cut into 10 μm thick sections. After deparaffinating in xylene and ethanol, the sections were treated with 10 μg/mL proteinase K for 20 min at 37°C. The sections were incubated with prehybridization solution, which was prepared by diluting salmon essence DNA with hybridization buffer. Next, the sections were incubated with hybridization buffer containing DIG-labeled riboprobes at 42°C overnight. Then, the sections were washed with decreasing concentrations of sodium citrate (SSC) buffer to remove any unbound probe and incubated with biotin-labeled anti-digoxigenin antibody (Cat#AR0147, BOSTER Biological Technology) for 60 min at 37°C. HRP Conjugated Streptavidin (BA1088, BOSTER Biological Technology) and TSA reagents (Cat# PN1004, PN1006, PINUOFEI Biological Technology) were

applied to visualize the signals. Finally, the tissue sections were counterstained with DAPI for 10 min. Sections were captured using a fluorescence microscope-Axio Imager Z2 (ZEISS, Oberkochen, Germany).

Quantitative real-time PCR (qRT-PCR)

Total RNA of mouse limbal tissues was isolated using TRIzol reagent (Cat#15596-026, Thermo Fisher Scientific) and converted to cDNA using the FastKing RT Kit (Cat#KR116, TIANGEN) following the manufacturer's instructions. qRT-PCR was carried out using the cDNA and SYBR qPCR Master Mix (Cat#Q311-02, Vazyme Biotech) by the LightCycler 480II System (Roche, Indianapolis, IN, United States). The cDNA levels were normalized against GAPDH transcripts to asses the relative mRNA levels using the $2^{-\Delta\Delta CT}$ method.

RNA sequencing (RNA-seq)

One week after topical injection of the antagonist, the mice were euthanized and the eyeballs were extracted. The corneal and corneoscleral tissues were removed on ice. Limbal tissues were quickly dissected and placed in RNAlater reagent (Simgen, Hangzhou, China) for RNA isolation. Each sample contained three to five independent repeated mice limbal tissues, and samples of each group were in triplicate. The Illumina NovaSeq 6000 sequenator (Illumina, San Diego, CA, USA) was used to perform the RNA-seq. The results were analyzed by RiboBio Co., Ltd. (Guangzhou, China). Differential expression analysis and KEGG analysis were performed. The differentially expressed genes were selected using the following thresholds: >2.0-fold change, *q*-value <0.05. We have uploaded the RNA-seq data to the GEO database.

QUANTIFICATION AND STATISTICAL ANALYSIS

GraphPad Prism software (version 8.0, GraphPad Software Inc., La Jolla, CA, USA) was used to perform statistical analyses. Comparisons between two groups were analysed using unpaired two-tailed Student's *t* test. Comparisons between multiple groups were assessed with one-way analysis of variance (ANOVA). All data are shown as the mean ± SEM. Data were considered statistically significant at $p < 0.05$.